Erratum

Accelerometer tags: detecting and identifying activities in fish and the effect of sampling frequency

Franziska Broell, Takuji Noda, Serena Wright, Paolo Domenici, John Fleng Steffensen, Jean-Pierre Auclair and Christopher T. Taggart

10.1242/jeb.088336

There was an error published in *J. Exp. Biol.* **216**, 1255-1264.

The author affiliations for Paolo Domenici and John Fleng Steffensen were incorrectly displayed. The correct version is given below.

Franziska Broell[1,*], Takuji Noda[2], Serena Wright[3,4], Paolo Domenici[5], John Fleng Steffensen[6], Jean-Pierre Auclair[1] and Christopher T. Taggart[1]

[1]Department of Oceanography, Dalhousie University, 1355 Oxford Street, Halifax, NS, Canada, B3H 4R2, [2]Department of Social Informatics, Graduate School of Informatics, Kyoto University, Yoshidahonmachi, Kyoto 606-8501, Japan, [3]CEFAS Laboratory, Pakefield Road, Lowestoft NR3 0HT, UK, [4]Department of Biosciences and Geography, Swansea University, Singleton Park, Swansea SA2 8PP, UK, [5]CNR-IAMC, Istituto per l'Ambiente Marino Costiero, Località Sa Mardini, 09072 Torregrande-Oristano, Italy and [6]Marine Biological Laboratory, University of Copenhagen, Strandpromenaden 5, 3000 Helsingør, Denmark

*Author for correspondence (franziskabroell@dal.ca)

We apologise to the authors and readers for any confusion that this error may have caused.

The Journal of Experimental Biology 216, 1255-1264

doi:10.1242/jeb.077396

RESEARCH ARTICLE

Accelerometer tags: detecting and identifying activities in fish and the effect of sampling frequency

Franziska Broell[1,*], Takuji Noda[2], Serena Wright[3,4], Paolo Domenici[5], John Fleng Steffensen[6], Jean-Pierre Auclair[1] and Christopher T. Taggart[1]

[1]Department of Oceanography, Dalhousie University, 1355 Oxford Street, Halifax, NS, Canada, B3H 4R2, [2]Department of Social Informatics, Graduate School of Informatics, Kyoto University, Yoshidahonmachi, Kyoto 606-8501, Japan, [3]CEFAS Laboratory, Pakefield Road, Lowestoft, NR3 0HT, UK, [4]Department of Biosciences and Geography, Swansea University, Singleton Park, Swansea SA2 8PP, UK, [6]CNR-IAMC, Istituto per l'Ambiente Marino Costiero, Località Sa Mardini, 09072 Torregrande-Oristano, Italy and [5]Marine Biological Laboratory, University of Copenhagen, Strandpromenaden 5, 3000 Helsingør, Denmark

*Author for correspondence (franziskabroell@dal.ca)

SUMMARY

Monitoring and measuring the behaviour and movement of aquatic animals in the wild is typically challenging, though micro-accelerometer (archival or telemetry) tags now provide the means to remotely identify and quantify behavioural states and rates such as resting, swimming and migrating, and to estimate activity and energy budgets. Most studies use low-frequency (≤32 Hz) accelerometer sampling because of battery and data-archiving constraints. In this study we assessed the effect of sampling frequency (aliasing) on activity detection probability using the great sculpin (*Myoxocephalus polyacanthoceaphalus*) as a model species. Feeding strikes and escape responses (fast-start activities) and spontaneous movements among seven different great sculpin were triggered, observed and recorded using video records and a tri-axial accelerometer sampling at 100 Hz. We demonstrate that multiple parameters in the time and probability domains can statistically differentiate between activities with high detection (90%) and identification (80%) probabilities. Detection probability for feeding and escape activities decreased by 50% when sampling at <10 Hz. Our analyses illustrate additional problems associated with aliasing and how activity and energy-budget estimates can be compromised and misinterpreted. We recommend that high-frequency (>30 Hz) accelerometer sampling be used in similar laboratory and field studies. If battery and/or data storage is limited, we also recommend archiving the events *via* an on-board algorithm that determines the highest likelihood and subsequent archiving of the various event classes of interest.

Supplementary material available online at http://jeb.biologists.org/cgi/content/full/216/7/1255/DC1

Key words: accelerometer tag, fish, behaviour, activity, feeding, escape, sampling frequency.

Received 12 July 2012; Accepted 13 November 2012

INTRODUCTION

Quantifying activity patterns and energy budgets among animal species is essential for the assessment and identification of basic life-history traits, habitat requirements and intra- and inter-specific interactions. Such information is also essential for parameterising ecosystem models and for advancing the informed management of commercially and recreationally valued fish species. Field observations of the behaviour and locomotion of aquatic animals in the wild are typically challenging, though micro-accelerometer (archival or acoustic and satellite telemetry) tags now provide the means to remotely monitor animals in the wild.

Accelerometer data can be used to quantify behavioural states and rates and to estimate energy expenditure in the field (Tsuda et al., 2006; Sato et al., 2007, Murchie et al., 2010; Payne et al., 2011; Whitney et al., 2010). In fish, acceleration metrics have been linked to heart rate and energy expenditure (Clark et al., 2010), spawning behaviour (Tsuda et al., 2006), activity (Kawabe et al., 2003a; Kawabe et al., 2003b) and, more recently, feeding behaviour (Føre et al., 2011). Generally, accelerometer tags continuously record data at some defined frequency or record a defined time-average of the data, which are either digitally stored or transmitted for subsequent post-processing. Post-processing is typically based on a broad categorization of the acceleration data (signal) using the average and maximum and/or minimum values of the acceleration (e.g. Murchie et al., 2010; O'Toole et al., 2010) or various frequency components thereof [e.g. fast Fourier transform (FFT) and wavelets (Sato et al., 2007; Sakamoto et al., 2009)], and often this is done subsequent to data transformation to various components of dynamic and static acceleration (Tanaka et al., 2001; Wilson et al., 2006; Gleiss et al., 2010). These signals and their variation (e.g. rates of change) are then combined to estimate activity and energy budgets or to classify various behaviours such as resting, swimming, etc. Many accelerometer studies involving fish (Kawabe et al., 2003a; Kawabe et al., 2003b; Tsuda et al., 2006; Murchie et al., 2010; O'Toole et al., 2010) employ sampling frequencies ≤32 Hz because of battery, data-storage and size constraints associated with commercially available tags. Observations obtained at such frequencies may allow for the identification of relatively simple behaviours such as resting and swimming or some complex behaviours such as spawning in large salmon (Tsuda et al., 2006) or mating in large sharks (Whitney et al., 2010). However, few studies address behaviours that in some fish species occur over short time scales of the order 100 ms; e.g. feeding strikes or escape responses

(Webb, 1978). These kinds of short-duration high-amplitude accelerations are essential components when estimating activity and energy expenditure. A link between accelerometer data and the movements associated with swimming bouts such as haphazard turns, predator–prey escape response or feeding strikes in fish has yet to be established. Video analyses, based on kinematic experiments focusing on such 'fast-start' behaviours in controlled laboratory conditions, have demonstrated relationships among acceleration metrics and high-resolution video records of movement (Harper and Blake, 1989; Harper and Blake, 1991; Domenici and Blake, 1997; Domenici et al., 2004). The above studies suggest that accelerometer data can be used to qualify and quantify more detailed variations in locomotion and behaviour, provided that the sampling frequency is sufficiently high (Harper and Blake, 1989). If the sampling frequency is too low, aliasing of the acceleration signal will occur (e.g. Oppenheim and Schafer, 1989; Sabin, 2008). Thus, behaviours associated with swimming, predator–prey escape response or feeding strikes may either be missed or misidentified. Because such short bursts of activity may result in anaerobic metabolic pathways being used and thus increase energetic demand (Goolish, 1991), the estimates of activity and energy budgets will at best be biased. To obtain estimates of state- and rate-inferred behaviours, and for confident estimation of activity patterns in any fish species, quantifying the species-specific effect of sampling frequency on the detection of locomotion associated with such behaviours is essential, especially if the activities occur over short time scales.

Given the above concerns, our study focused on two questions: (1) how can we statistically differentiate among various locomotion behaviours such as spontaneous movement, escape response and feeding strikes in fish; and (2) what is the effect of accelerometer sampling frequency on the detection and identification of these event classes, i.e. when does aliasing compromise detection and identification? We used a readily available and hardy species, the great sculpin (*Myoxocephalus polyacanthocephalus*), as our model fish to collect acceleration data and associated statistical parameters from a suite of activity trials to address the two questions. We then considered how appropriate sampling frequencies can be used in field studies to remotely monitor complex fish behaviour in a manner not previously possible.

MATERIALS AND METHODS

Study animals

Seven great sculpin (*Myoxocephalus polyacanthocephalus* Pallas 1814) ranging in size from 29.0 to 35.0 cm fork length (mean ± s.d.=31.8±2.0 cm) weighing between 560 and 940 g (mean ± s.d.=668.7±142.9 g) were collected using a beach seine at two locations on the southeast side of San Juan Island, Washington, USA, and were used in the activity trials conducted at Friday Harbor Laboratories. The fish were held in a 170 cm diameter outdoor tank with flow-through seawater maintained at 11±1°C (mean ± s.d.) and 1 m depth. Fish were acclimatized to the tank for at least 1 week prior to the tagging and the activity trials that took place over a 14 day period. After tagging, food was withheld to ensure a feeding response to the presence of live, wild-caught sandlance (*Ammodytes* spp.), a preferred prey type for sculpin based on preliminary food selection trials using multiple natural prey types. The use of dead prey was also tested, but it elicited unnatural feeding behaviour from the animals.

Accelerometer

An ORI-380D3GT micro-accelerometer (Little Leonardo, Tokyo, Japan) was used to record tri-axial acceleration. The accelerometer (±4 ***g***) sampling frequency was set at 100 Hz using a 12 bit resolution and 10 h data storage capacity. The accelerometer tag was 12 mm in diameter and 45 mm length, with a mass of 10 g (≤2% of fish fresh mass).

Activity trials

Fish anaesthetized with MS222 (80 mg l^{-1}) were measured for length and mass and were then tagged using Petersen Disk tags (Floy Tag, Seattle, WA, USA) 1 week prior to the feeding and escape activity trials. Two disk-tags, one forward and one aft of the centre of the first dorsal fin, were attached ~0.5 cm below the insertion point of the fin, a location assumed to be the least invasive and positioned at an attachment point closest to the centre of gravity, estimated (post-mortem, using a point balance) at 0.35 body lengths from the tip of the snout (supplementary material Fig. S1). The temporary (for trials) attachment of the accelerometer tag to the disk pair was accomplished using Velcro. We experienced no complications during the tagging procedure.

For each activity trial an individual fish was tagged with the accelerometer during transfer from the holding tank to an identical and adjacent trial tank where the water level was maintained at 0.5 m depth to ensure reliable video (see below). The transfer and tagging time ranged between 2 and 3 min, after which none of the animals showed signs of stress and all settled quickly in the trial tank. Fish were acclimated to the trial tank for 30 min prior to the start of the activity trials. For escape trials, an escape response was triggered at ~30 min intervals using the method of Domenici et al. (Domenici et al., 2004). Between nine and 15 escape responses were elicited and recorded for each fish. For feeding trials, five live sandlance were introduced to the tank to allow the fish to feed *ad libitum*. Depending on the responsiveness of the fish, between 12 and 22 feeding strikes (successful or not) were recorded per fish. Additionally, 10 spontaneous swimming events (haphazard turns, swimming, minor body movements when at rest) were recorded for each fish during the suite of trials. Activities were noted manually when visually observed, recorded using the accelerometer and video-recorded using a 30 Hz standard USB webcam (Microsoft LifeCam, VX-1000 and H264 Webcam 3.83 software, Redmond, WA, USA) located 2.6 m above the tank bottom. Manual notation (computer clock), accelerometer and video recording were synchronized prior to a set of activity trials. The data used for analyses were based on a total of 160 h of accelerometer recordings among the activity trials.

The care and sampling protocol for the tagging surgery and live predator–prey experiments in this study was approved by the University of Washington in accordance with Institutional Animal Care and Use Committee standards (permit no. 4238-04).

Acceleration data extraction

The timestamps on the accelerometer and the video recording were used to localize acceleration events. Using visual observations of locomotion, the events were assigned a class, either spontaneous (S) or 'fast-start' (FS) (Domenici and Blake, 1997), where the latter was further divided into feeding (F) and escape (E) activity classes. For each observed fast-start event and 10 randomly selected spontaneous events, a 1 s period of the acceleration record was extracted and centred on the maximum acceleration. This 1 s interval is hereafter referred to as an 'event'. The length of the event period was chosen after video observations revealed that all observed fast-start events occurred within that period.

The acceleration data were processed as three-dimensional acceleration (lateral, longitudinal and vertical) here referred to as the *x*-, *y*- and *z*-axes, and the magnitude of acceleration (MA), which

is the vector norm, not corrected for gravitational acceleration: $MA=\sqrt{(x^2+y^2+z^2)}$. To avoid unnecessary complications due to the directionality of events in the lateral *x*-axis, the events were standardized such that the maximum acceleration amplitude in the *x*-axis was positive. Event data (N_{DS}=70, N_{DE}=82, N_{DF}=105) were randomly divided into two subsets, the training subset (N_{TS}=40, N_{TE}=51, N_{TF}=53), which served to establish parameter threshold values, and the validation subset (N_{VS}=30, N_{VE}=31, N_{VF}=52), which was treated as a independent data set with the purpose of testing parameter efficiency and the effect of sampling frequency (aliasing). Statistical analyses and algorithm computations were performed using R Statistical Computing Software (version 2.13.0, R Foundation for Statistical Computing, Vienna, Austria) and MATLAB 7.12 (The MathWorks, Natick, MA, USA).

Discrete parameter analysis

Our goal was to establish a parameter or a parameter set capable of detecting events and identifying the activities with minimal variation within and amongst individuals, that is size-independent, and independent of values that depend on the accelerometer mounting position and the size of the fish (e.g. maximum acceleration). Parameters from the frequency domain (using spectral and wavelet analysis), the probability domain (using the probability density function, and population parameters such as mean, maximum and variation in acceleration) and the time domain (using autocorrelation and pattern descriptive parameters, i.e. integral, derivative) were examined for their utility in detecting and identifying activity in the acceleration records. A systematic signal processing approach, as conceptualized in Fig. 1, was developed to: (1) detect fast-start events using an event detection parameter (Φ), and (2) identify fast-start events as being either feeding or escape activity using a parameter set, $\Omega=[\omega_1, \omega_2,..., \omega_i]$, where ω_i is the *i*th identification parameter in the Ω set. Suitable parameters were established using the entire event data set. Threshold values for significant parameters were then determined using an optimization routine based on the training subset. Finally, the efficiency of the established parameters and the effect of sampling frequency were determined using the validation subset.

Establishing suitable parameters

Procedure

All parameters identified as being potentially useful were tested for average differences between spontaneous and fast-start events and between activity classes for all fish in the aggregated (Student's *t*-test for normally distributed data, Wilcoxon signed-rank test otherwise) and the disaggregated (individual fish) data. Parameters were rejected if differences between event or activity classes were insignificant for either the aggregated or the disaggregated data.

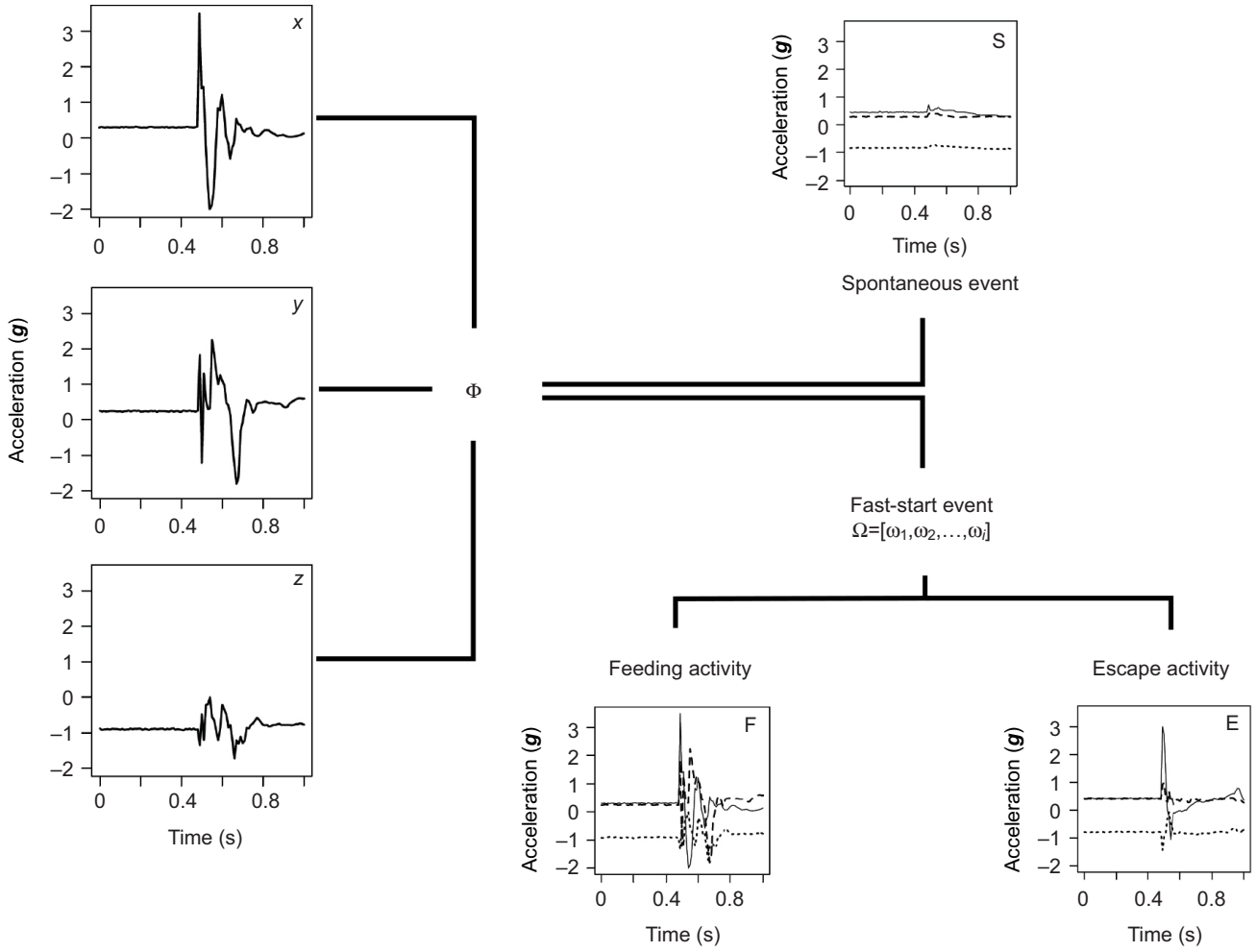

Fig. 1. Schematic representation of the use of tri-axial (*x*, lateral; *y*, longitudinal; *z*, vertical) acceleration (*g*) time series to first detect (Φ parameter) and then identify (Ω parameter set) spontaneous (S) events, and feeding (F) and escape (E) activities in sculpin with representative event acceleration series for illustration.

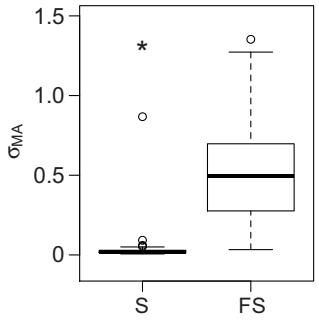

Fig. 2. Box and whisker plots of standard deviation of the magnitude of acceleration (σ_{MA}) for seven different great sculpin from spontaneous (S, N_S=71) and fast-start events (FS, N_{FS}=187) using aggregate fish based on the entire data set. The box illustrates the inter-quartile range (IQR), the bar the median, the whiskers ±1.5 IQR and the open circles the outliers. The asterisk (*) indicates that the population mean of spontaneous events is lower than that of fast-start events (Wilcoxon signed-rank test, P<0.0001; see supplementary material Table S1 for details).

Parameters derived from the frequency and probability domains suffered from low data density. For example, escape activity, typically occurring over an average of 250 ms, contain ~25 data values when sampled at 100 Hz. Thus, these domains were suboptimal and were dismissed. Parameters describing the 'shape' of the event, such as the acceleration integral or the acceleration derivative, were tested and dismissed because no difference between activity classes was determined. Furthermore, average acceleration values for MA (the vector norm), or individual components thereof, were not different between activities.

Detection parameter Φ

The most robust and efficient detection parameter for the fast-start movements was the standard deviation of the vector norm of acceleration, σ_{MA}. The standard deviation was significantly smaller for spontaneous than for fast-start events (Fig. 2, supplementary material Table S1). Maximum acceleration of the vector norm was also greater among the fast-start events; however, it was dismissed because of its dependency on fish size and the attachment location of the accelerometer (see Discussion). This parameter was considered sufficient to differentiate between spontaneous and fast-start events.

Identification parameters Ω

Six significant parameters (ω_1, ..., ω_6) that were different between fast-start event activity classes were determined following the procedure outlined above and as summarized in Fig. 3 and supplementary material Table S1. For parameters ω_1 to ω_4, a statistical property of acceleration in the x-axis differed from that in the y-axis for escape activity, but not for feeding activity. For example, ω_1 was based on the standard deviation, i.e. $E[\sigma_x-\sigma_y]>0$ for escape events and $E[\sigma_x-\sigma_y]=0$ for feeding events. The other parameters were based on the maximum acceleration (ω_2), the range of the acceleration data (ω_3) and the root mean square (ω_4). Parameter ω_5 was based on the sum of the autocorrelation coefficient τ at lags 1 to 3 in MA, which was significantly greater in escape events than in feeding events. Parameter ω_6 was based on the Spearman correlation coefficient, ρ, between the x- and y-axes, which was greater in feeding than in escape events.

Establishing parameter threshold values

For the Φ and each of ω_1, ..., ω_6, a threshold value and parameter weights were empirically determined using an optimization routine based on the test data subset. This routine was designed to find cut-off values, v_k (where k=1, ..., 7), which maximize both the percentile of the observed parameter values of one event/activity class falling below v_k, and the percentile of the observed values falling above v_k of the other event/activity class (Table 1). For example, the detection

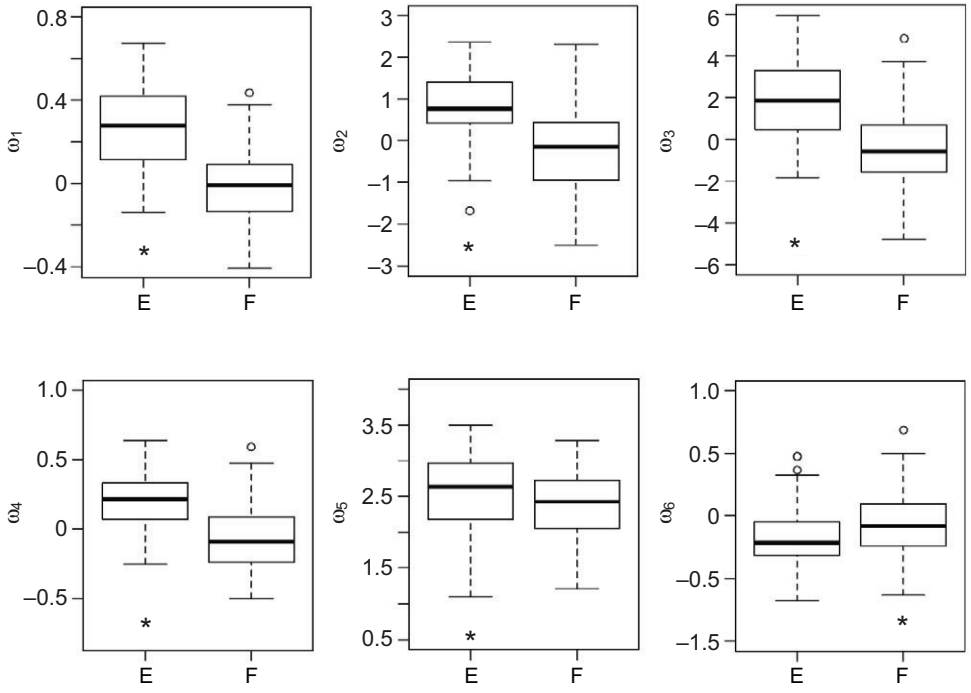

Fig. 3. Box and whisker plots illustrating differences between escape (E) and feeding (F) activities for each parameter ω_i, where the box illustrates the inter-quartile range (IQR), the bar the median, the whiskers ±1.5 IQR and the open circles the outliers. The asterisk (*) indicates that parameter values are significantly higher (P<0.05) in E than F for all except ω_6, where the reverse is the case.

Table 1. Summary of the significance of parameter threshold-value tests

Parameter	Event/activity class	Testing hypothesis	Weight (C)
Φ	FS	H_A: $E[\sigma_{MA}] > 0.2$*	0.989
	S	H_A: $E[\sigma_{MA}] < 0.2^{\dagger}$	0.949
ω_1	E	H_A: $E[\sigma_x - \sigma_y] > 0.08^{\dagger}$	0.714
	F	H_A: $E[\sigma_x - \sigma_y] < 0.08$*	0.700
ω_2	E	H_A: $E[A_{max,x} - A_{max,y}] > 0.31$*	0.755
	F	H_A: $E[A_{max,x} - A_{max,y}] < 0.31$*	0.750
ω_3	E	H_A: $E[R_x - R_y] > 0.54$*	0.673
	F	H_A: $E[R_x - R_y] < 0.54$*	0.670
ω_4	E	H_A: $E[RMS_x - RMS_y] > -0.01^{\dagger}$	0.642
	F	H_A: $E[RMS_x - RMS_y] < -0.01^{\dagger}$	0.652
ω_5	E	H_A: $E\left[\sum_{m=1}^{3}\tau_m\right] > 2.7^{\dagger}$	0.611
	F	H_A: $E\left[\sum_{m=1}^{3}\tau_m\right] < 2.7$*	0.625
ω_6	E	H_A: $E[\rho_{xy}] < -0.14$*	0.653
	F	H_A: $E[\rho_{xy}] > -0.14$*	0.648

$E[\cdot]$ is the hypothetical expectation for spontaneous (S) and fast-start (FS) events and feeding (F) and escape (E) activities all based on the number of events and activities in the training subset data.

Threshold values were tested using Student's t-test or Wilcoxon sign-rank, with significance indicated by * or †, respectively.

The parameters include the standard deviation of the acceleration vector norm, σ_{MA} (Φ), and the parameter set Ω, including the standard deviation, σ, in the x or y acceleration axes (ω_1); the maximum acceleration amplitude, A_{max}, in the x or y axes (ω_2); the range in acceleration, R, in the x or y axes (ω_3); the root mean square, RMS, in the x or y axes (ω_4); the sum of autocorrelation coefficients, τ, for lags 1, 2, 3 in the vector norm (ω_5); and the correlation coefficient, ρ, between the x and y axes (ω_6).

The subscripted parameter weights, C, are the number of events where the parameter threshold applies, expressed as a proportion.

parameter σ_{MA} was greater than the optimized threshold value, v_1, of 0.2 for fast-start events and <0.2 for spontaneous events. Hence the threshold of 0.2 was of significance in correctly detecting a fast-start event. This example applied for each of the ω parameters accordingly (Table 1). The optimized percentiles represent the empirical weight (C_{Φ}, $C\omega_{i,E}$, $C\omega_{i,F}$; Table 1) of each parameter for a given threshold, which can be interpreted as a confidence in each parameter for each event class. For example, the detection parameter σ_{MA} had a weight of 0.989 for fast-start events, which means that 98.9% of all fast-start events exhibited a standard deviation that was greater than the optimized threshold.

Testing parameters

Procedure

Parameter efficiency was tested using the validation data subset. These data stem from five 10 h continuous acceleration records (1.8×10^7 data values) spanning numerous spontaneous and 83 observationally verified fast-start events. We used these data to determine the detection probability (fast-start events), the identification probability (feeding or escape activity) of detected events and the performance of the individual parameters. We also examined the effect of accelerometer sampling frequency on detection and identification probability (see Sampling frequency below).

Detection probability

The fast-start detection probability was established using a fast-start detection algorithm. This is a sliding window algorithm that calculated the standard deviation for each 1 s window of the MA time series and, based on that value (compared with the threshold v_1; Table 1), allocated an event ID ('fast-start event', 'spontaneous event') to the acceleration window. The detection, $P(D|R)$, and false detection, $P(D|NR)$, probabilities were then established by comparing the fast-start events detected by the algorithm with the observed ('real') events, where D indicates an event detected, R is a real event and NR is a 'not real' event.

Identification probability

For each 1 s (detected $\cap$ real) event from the fast-start detection algorithm, the parameter set Ω was calculated. The identification (F, E) was obtained from a sum of diagnostic indicators ('feeding' or 'escape') for every parameter weighted by their confidence (Table 1). To determine the identification probability (number of correctly identified events/number of real events), the identification (F, E) was compared with the real event identity (F, E). We then estimated the probability of correctly identifying a detected and real event $P(I\cap D|R)$ and the equivalent probability for escape, $P(I_E\cap D_E|R_E)$, or feeding events, $P(I_F\cap D_F|R_F)$, where I indicates a correct identification. These probabilities determined the performance of the algorithm (detection and identification). Given detection, the probabilities of correct identification, $P(E|E)$ and $P(F|F)$, and misidentification, $P(F|E)$ or $P(E|F)$, were also determined for each activity class and parameter, and were used to assess the performance of the identification parameters.

Sampling frequency

Various sampling frequencies were considered to assess their effect on the ability of the algorithm to correctly detect events and identify activities. The lower-frequency time series were obtained from the 100 Hz data by subsampling the original acceleration record to generate an array of every possible sub-sampled series. For example, four different 25 Hz series were generated by starting from each of the first through the fourth datum and keeping every fourth subsequent datum. Multiple lower-frequency sets of series from 50 to 3.33 Hz were generated similarly, by starting with the second through 30th datum in the original series. To avoid additional biasing in the lower-frequency analyses, parameters, thresholds values and weights (as detailed in Establishing suitable parameters and Establishing parameter threshold values above) were re-assessed for each sampling frequency. Consequently, 'dynamic' threshold values for spontaneous and fast-start events and feeding and escape activities and their associated 'dynamic' weights were generated as a function of frequency.

The detection parameter, Φ, remained significant in differentiating fast-start and spontaneous events for all sampling frequencies considered. The previously determined threshold also applied across all the decreasing sampling frequencies, with a slight decrease in weights (ranging from 0.95 to 0.85).

For the set of identification parameters, Ω, only ω_1 to ω_4 remained applicable for differentiating between escape and feeding events across the decreasing sampling frequencies (Fig. 4). Parameters ω_5 and ω_6 did not provide sufficient confidence ($\leq$0.5) and were therefore removed from the analysis. For significant parameters, a dynamic threshold and dynamic weights were established (Fig. 5). The dynamic weights for the identification parameters also decreased with decreasing frequencies. Using the recalculated thresholds and weights, detection and identification probabilities for each sampling frequency were established, as above. Because the subsampling procedure provided multiples series at each simulated frequency, the detection/identification probability was described by the average detection probability and one standard deviation for all sampling frequencies <100 Hz.

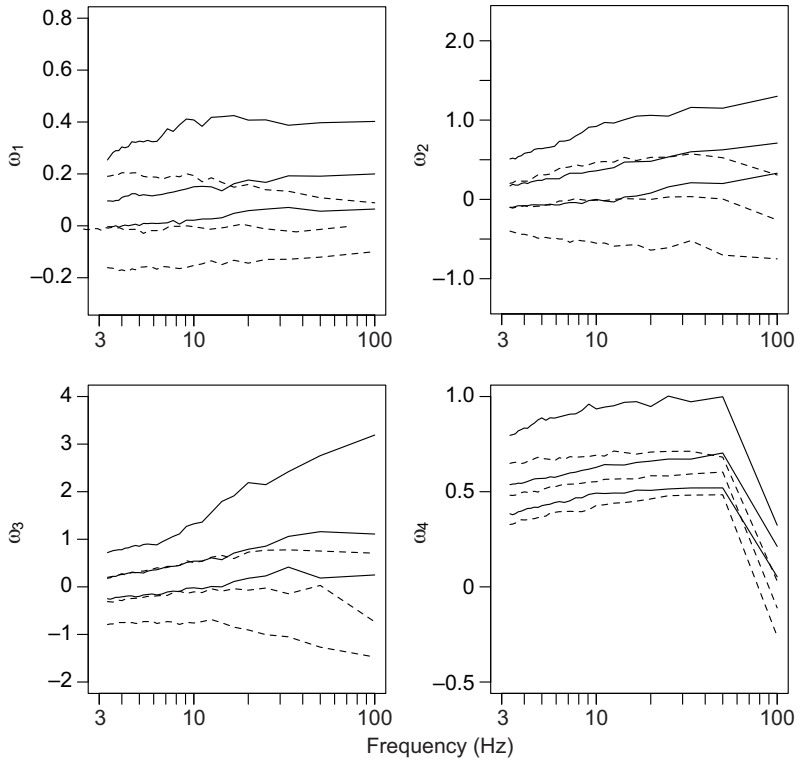

Fig. 4. Median values with upper and lower quartiles for parameters ω_1, ω_2, ω_3 and ω_4 as a function of sampling frequency calculated using the entire event data set for escape (solid lines) and feeding (dashed lines) activities (see Table 1) on a semi-log scale.

RESULTS

Parameter performance at 100 Hz

The detection parameter Φ was highly efficient, with a $P(D|R)$ of 0.89 and a $P(D|NR)$ of 0, and specifically a $P(D_E|R_E)$ of 0.94 and a $P(D_F|R_F)$ of 0.85. The identification parameter set, Ω, was also efficient, with a $P(I \cap D|R)$ of 0.77, and specifically with a $P(I_E \cap D_E|R_E)$ of 0.91 and a $P(I_F \cap D_F|R_F)$ of 0.69. The efficiencies of each parameter in identifying escape or feeding, given detection, were variable (Fig. 6). The quadrangle in Fig. 6 allows a comparison of efficiencies among parameters and the entire parameter set, where perfect event identification is represented on the vertical axis that ranges from $P(E|E)=1$ and through zero to $P(F|F)= 1$; i.e. a parameter

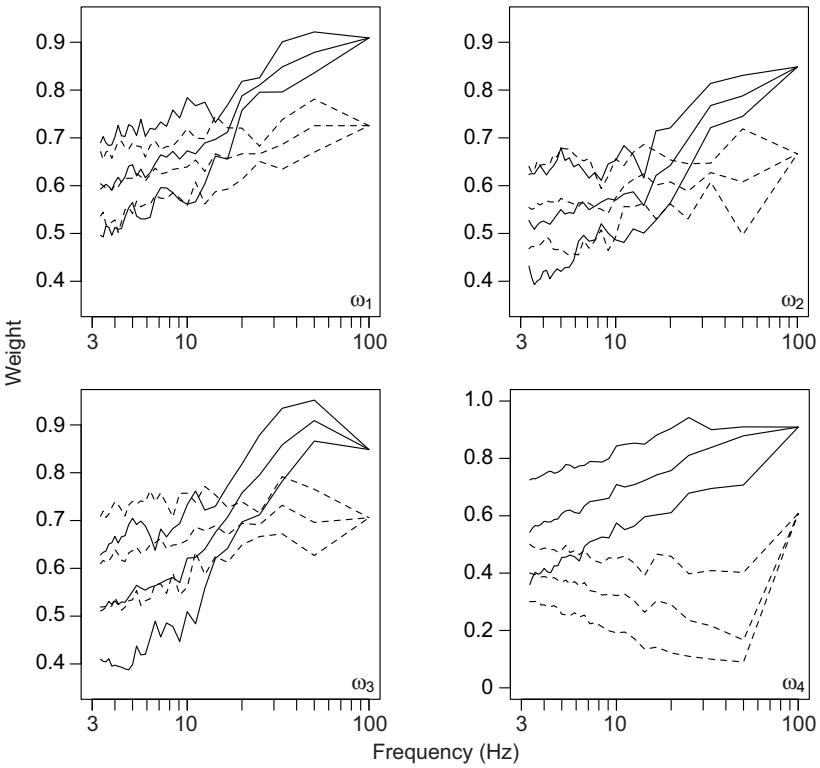

Fig. 5. Median (±1 s.d.) weights for parameters ω_1, ω_2, ω_3 and ω_4 calculated using the entire event data set for escape (dashed lines) and feeding (solid lines) activities as a function of sampling frequency (see Table 1) on a semi-log scale.

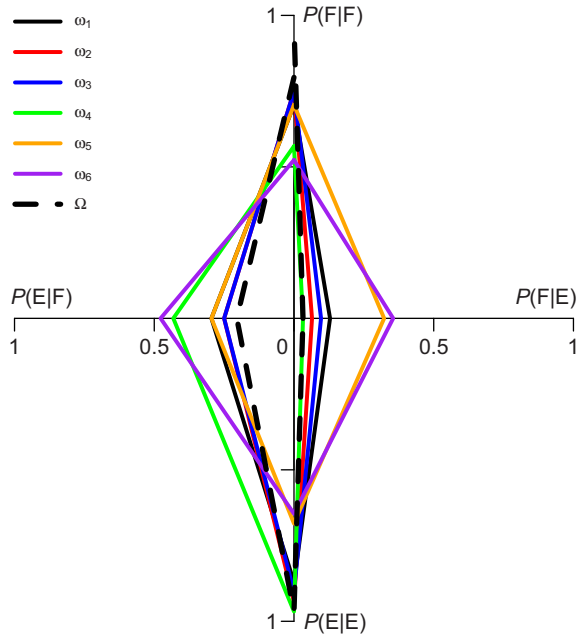

Fig. 6. Colour-coded quadrangle representation of the parameter efficiency space showing the probabilities of activity identification for each of the parameters in Ω (solid colours) and the Ω parameter set (dashed black line). Correct identifications are represented by the vertical between *P*(EIE) and *P*(FIF), and misidentifications are represented by the horizontal between *P*(EIF) and *P*(FIE).

line on the axis reflects a 100% probability of correctly identifying both escape and feeding vents. Similarly, incorrect identification is represented on the horizontal axis that ranges from $P(E|F)=1$ and through zero to $P(F|E)=1$. While the full parameter set, Ω, was very efficient in the identification of escape events with $P(E|E)=0.97$, it was less efficient in identifying feeding events, with $P(F|F)=0.79$ (Fig. 6). This asymmetry in performance was also evident for most individual parameters (ω_1, ω_2, ω_3, ω_4), where $P(E|E)>P(F|F)$. In turn, ω_5 performed poorly for escape event identification while being efficient in identifying feeding events, and ω_6 seemed generally poor. However, neglecting ω_6 led to a noticeable decrease in the identification efficiency. This shows that less accurate parameters can compensate for diagnostic errors introduced by other parameters when there is low agreement among the high confidence parameters.

Identification and detection rates

The average detection and identification probabilities and their standard deviations, over the range of sampling frequencies examined, are provided in Fig. 7. The detection and identification rates are the probabilities of detection, $P(D|R)$, and identification given detection, $P(I\cap D|R)$, as a function of sampling frequency. We considered this to be the most appropriate tool for assessing the total effect of sampling frequency because it incorporates the cumulative effect of sampling frequency on both detection and identification. The detection rate decreased hyperbolically while identification rates decreased logarithmically (Fig. 7A) with decreasing frequency. At 100 Hz, 89% of all fast-start events were detected and 77% were properly identified. The class-specific identification probability was 69% for feeding and 91% for escape (Fig. 7B). Detection decreased to 50% near 4 Hz and identification near 14 Hz for all fast-start events combined, or near 16 Hz for feeding and 7 Hz for escape separately. At 30 Hz, the maximum

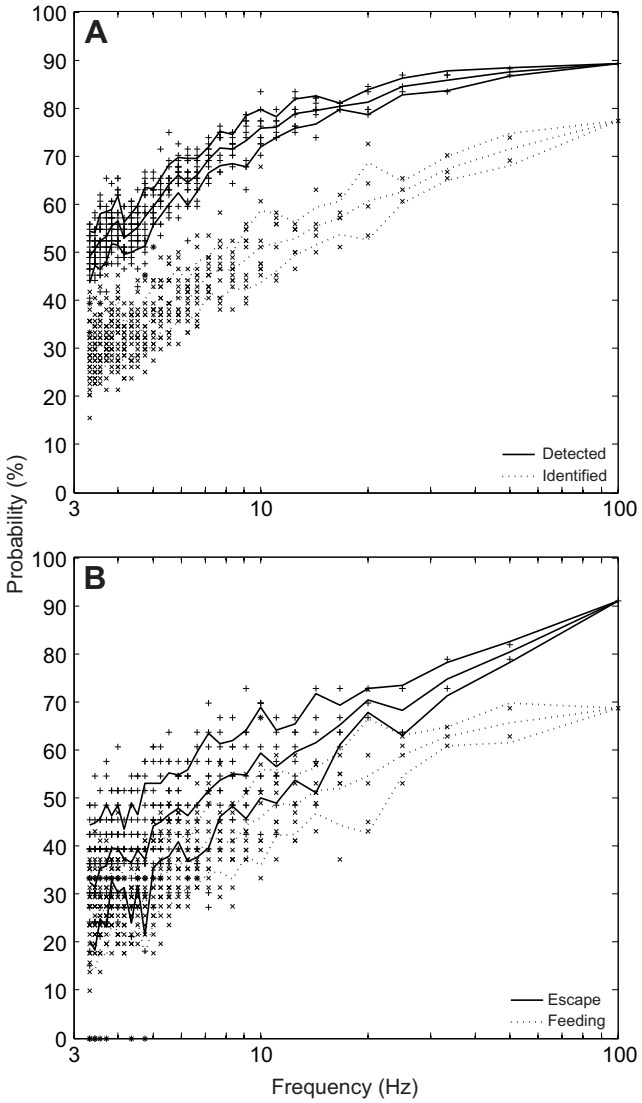

Fig. 7. Cumulative detection and identification algorithm efficiency expressed as a probability (%) as a function of sampling frequency on a semi-log scale for (A) event detection (pluses) and identification (crosses) and (B) identification of escape (pluses) and feeding (crosses) activity.

frequency typically used in the field, 85% of the events were detected and 67% were properly identified. Class-specific identification rates decreased to 62% for feeding and 74% for escapes at this frequency.

DISCUSSION

As best as we can determine, this is the first study that uses a high-frequency accelerometer tag to detect and identify different types of behavioural events in fish with relatively high efficiencies of ~90% for event detection, ~80% for event identification, and between ~70 and ~90% for feeding and escape activities, respectively. We have shown that these efficiencies can be achieved using a relatively simple set of statistical parameters drawn from the time and probability domains of the acceleration record without the need to pre-process (filter) the acceleration signal. Apart from the generally descriptive and cautionary work of Ropert-Coudert and Wilson (Ropert-Coudert and Wilson, 2004) and the metabolic studies of Halsey et al. (Halsey et al., 2009), this also appears to be the first study that quantitatively demonstrates that achieving the

above efficiencies is a function of the accelerometer sampling frequency, i.e. decreased sampling frequency results in decreased event detection and identification probability.

Accelerometers are often used in studies where the sampling frequency of the device depends on the technology (power, storage, etc.) and the size of the animal. Securing high-frequency data generally implies a larger battery requirement and a larger storage capability, each of which increase the tag dimensions. They are typically attached to animals in the field, retrieved at some later time and the data are analysed. In fish, simple parameters such as tail beat frequency and general activity are readily available, yet constrained sampling frequencies will alias the acceleration signal and thus compromise the ability to detect activities or movements that occur over short time scales.

Parameters

The suite of parameters we established was selected by statistical significance with some biological underpinnings. For the giant sculpin, acceleration variation in the *y*- and *z*-axes provided a smaller contribution to the vector norm in spontaneous movements. For example, steady swimming was dominated by sinusoidal lateral acceleration (tail beat) with little acceleration in the longitudinal and vertical axes. As shown above, fast-start movements resulted in accelerations and decelerations over milliseconds in all three axes. Not surprisingly, these movements exhibited greater variation in the vector norm (MA) and became manifest in the detection parameter σ_{MA}. To identify the fast-start events, we used six parameters, four of which were generally robust and of use at sampling frequencies <100 Hz (Fig. 4). While the detection parameter, Φ, and only one identification parameter (ω_5) were based on the vector norm [comparable to overall dynamic body acceleration; see Wilson et al. (Wilson et al., 2006) and Halsey et al. (Halsey et al., 2009), without a correction for gravity], these other four identification parameters were related to inter-axial (*x*- and *y*-axes) comparisons. When based on the vector norm, they failed in event identification. While this indicates that MA may be suitable for some applications, our results demonstrate that valuable information is lost when the three axes are combined into one metric, especially when investigating short time-scale movement. Interestingly, parameters for MA or axis-specific metrics such as the acceleration integral or derivative, or average acceleration, have been used for physiological classification purposes (Clark et al., 2010), for both physiological and activity classification (Murchie et al., 2010; O'Toole et al., 2010) and for metabolic studies (Payne et al., 2011). However, these parameters were incapable of detecting or identifying events and/or activities in our study due, in part, to large intra-individual variation, which was too large to establish a significant difference between events or activities. Perhaps more importantly, relatively infrequent events associated with substantial changes in acceleration over short time scales, if averaged, may become undetectable and unidentifiable, and increasingly so with the width of the averaging window and with decreasing sampling frequency. This implies that physiological and (or) metabolic estimates based on data manipulations, such as averaging, may be compromised, especially if fast-start activities comprise a substantial proportion of the behavioural repertoire, e.g. in ambush predators.

Limitations on parameters

The family of identification parameters achieved high rates of event detection (89%) and identification (77%) for a sampling rate of 100 Hz. While powerful in the correct identification of escape events (>90%), 20% of feeding events were misidentified as escape events. This is likely explained by feeding events being more variable than escape events because they are influenced by prey direction and distance, as well as by strike success. This would also be consistent with the variation in most parameters being greater among feeding events than among escape events. Preliminary examinations of parameter interactions (not presented here) did not improve the efficiency of the parameter set. Additionally, the activity identification of feeding events was more limited by feeding event detection (85%), which was lower than that for escape events (94%).

Many studies have addressed the effect of size on fast-start acceleration in fish, especially maximum acceleration (A_{max}) (Webb, 1976; Webb, 1978; Domenici and Blake, 1997; P.D., unpublished); therefore, in our study we kept the size of the animals relatively constant. The detection parameter was specifically designed to exclude values such as A_{max} (although significantly different between spontaneous and fast-start events) to avoid the influence of size, and fortuitously the attachment location and/or angle (Tsuda et al., 2006). The parameters ω_1, ..., ω_4 were based on inter-axial differences (0 or $\neq$0) and we assumed that if acceleration values (increase or decrease) or magnitude changed with size, the relative differences of axes within the animal would be near constant. Correlation parameters (ω_5, ω_6), which were not based on inter-axial comparisons but on inter-event comparisons, may have been subject to changes in threshold values accordingly to animal size.

Compared with most other fish, the sculpin is limited in terms of movement, especially in the vertical direction, and this most likely explains the negligible contribution of the vertical axis to the full parameter set, Ω. If a fish species that moves more in the vertical domain had been used, such as a cruise predator, we would expect vertical acceleration to make a greater contribution to the parameter set (e.g. Kawabe et al., 2003a). Fast-start event detection may be more complex if the vertical acceleration contribution to spontaneous movement increased, which could decrease the power of the standard deviation as a stand-alone detection parameter and thus other parameters may be required to detect fast-start events.

We neglected the statistical identification of simple locomotion, such as resting or swimming, because comparable acceleration studies in fish have shown that FFT analyses will detect and identify these movements (Kawabe et al., 2003a; Whitney et al., 2010).

Sampling frequency

The issues associated with aliasing are well known in the time series analysis and signal processing literature (Oppenheim and Schafer, 1989). However, in the field of animal accelerometry, the question of sampling frequency has received comparatively little attention. Given that fast-start events typically span a range of 200–700 ms in animals of comparable size (Domenici and Blake, 1997), high sampling rates are required to adequately capture these events in the accelerometer record. We have shown that detection and identification rates of these events decrease significantly with decreasing sampling frequency, i.e. the signals of interest are increasingly aliased at lower frequencies.

We are unaware of any accelerometer study on aquatic organisms that employs accelerometer tags sampling at frequencies greater than 32 Hz. Sampling at such low frequencies may be justified for large animals such as whales and large sharks, where observable behaviour occurring over milliseconds is unlikely (Gleiss et al., 2009; Gleiss et al., 2011; Whitney et al., 2007; Whitney et al., 2010; Goldbogen et al., 2011), but for smaller species such as trout, salmon and flatfish (Kawabe et al., 2003a; Kawabe et al., 2003b; Tsuda et al., 2006),

a higher accelerometer sampling frequency will likely prove informative, as shown above. The decrease in event detection probability at low sampling frequencies may be acceptable (a sampling frequency of 20 Hz results in a detection probability of ~60% of fast-start events), yet the identification of the event type decreases rapidly, especially for feeding events, where only 60% of events are properly identified at 30 Hz. Coincidentally, <30 Hz is a typical sampling frequency for archival or acoustic transmitter tags used in most experiments cited above and thus some information may be compromised. Although the foci of such studies are large time-scale movements (e.g. tail beat frequency) and the quantification of general activities (resting *versus* swimming), short-burst acceleration events such as feeding and escape are energy intensive and thus make crucial contributions to activity and/or energy expenditure. It is therefore essential to be able to detect the events to avoid compromised activity budgets and related physiological estimates. This will apply in the laboratory and perhaps more so in the wild, where there is virtually no knowledge of how often fast-start events occur. Further, activity detection and identification in the wild, particularly with the differentiation of successful and unsuccessful feeding events, could be especially useful in estimating energy budgets, especially the temporal (day *versus* night) and spatial variation (e.g. depth-structured temperature gradients) in energy expenditure and gain (feeding), for which we also know little. For example, methodologies similar to those developed here, used in combination with depth or location sensors, could allow the determination of feeding grounds with important implications for various habitat management strategies (Cartamil and Lowe, 2004).

Technological constraints do not, as yet, easily allow for conventional accelerometer tags to sample at high frequencies for durations greater than several days. However, we argue that continuing advances in micro-technology should result in decreased size and more efficient accelerometer units (in terms of battery, storage, micro-processors) that will allow for increasing sampling frequencies, onboard processing, greater storage and longer duration. Until such time, we recommend that accelerometer field studies focusing on behaviour, activity, physiological costs, kinematics, etc. include phases of laboratory experiments with high-resolution, short-duration accelerometer tags as shown here to quantify: (1) the parameters of interest and (2) the essential sampling frequencies. While many studies have demonstrated the use of accelerometers to link some simple and some complex behavioural traits and animal locomotion to acceleration in field applications, for short time-scale events it will be necessary to establish *a priori* the link between the behaviour or physiology and acceleration and to do so at the appropriate sampling frequency.

Future in tag micro-processing

On-board micro-processing, such as that already used in some accelerometer tags, decreases the amount of storage of high-resolution data to be archived or transmitted. Based on this study, micro-processing technology could be advanced to the point where algorithms determined *a priori* (e.g. activity detection and identification) constantly calculate the key parameters, allocate event IDs as they occur and store or transmit the data (see Føre et al., 2011), thus providing the *in situ* delivery of activities and behaviour over time. This would only be possible if micro-processing uses little power. Although this study cannot solve the technological issues around high-resolution accelerometers, it does address the consequences of aliasing when using low sampling frequencies. And though not all studies will require high-resolution accelerometers, we stress the importance of aliasing when embarking on field-tagging studies.

LIST OF SYMBOLS AND ABBREVIATIONS

A_{max}	maximum acceleration; subscript indicates the axis or MA
C	empirical weight associated with each parameter and event/activity class
D	event detected; subscript indicates event/activity class
E	escape activity
$E[.]$	expected value
F	feeding activity (attempted or successful feeding)
FFT	fast Fourier transform
FS	fast-start event (F or E)
I	event correctly identified; subscript indicates event/activity class
MA	magnitude of acceleration
N	sample size (subscript indicates data subset)
NR	not observed (real) event; subscript indicates event/activity class
$P(.\|.)$	conditional probability
R	observed event (real); subscript indicates event/activity class
S	spontaneous movement (haphazard turns, swimming, etc.)
t	time step
v_k	cut-off value (parameter threshold) for each of k parameters
x-axis	lateral
y-axis	longitudinal
z-axis	vertical
Ω	identification parameter set
ω_i	ith identification parameter (contained in Ω)
Φ	detection parameter
ρ	correlation coefficient
σ	standard deviation (subscript indicates axis)
τ	autocorrelation coefficient

ACKNOWLEDGEMENTS

We thank D. Willows, Director, and the staff of Friday Harbor Laboratories, University of Washington, USA, for their logistical support. We are grateful to J. Johansen for his contributions. We also thank two anonymous referees who contributed to the improvement of this manuscript.

AUTHOR CONTRIBUTIONS

F.B., T.N., S.W., P.D. and J.F.S. contributed to the design and execution of the experimental study. T.N. and S.W. extracted data from acceleration and video records and synchronized the data. F.B. designed, and implemented the statistical analyses of the acceleration data with insights from J.-P.A. and C.T.T. J.-P.A. contributed to signal processing and algorithm development. F.B. prepared the MS with advice on results and interpretation from C.T.T. All authors provided critiques on the research and the manuscript.

FUNDING

This work was supported by the OTN Canada – NSERC Strategic Network Grant [NETGP 375118-08 to F.B. and C.T.T.], by the Fisheries Society of the British Isles [to S.W.]. Funding was also provided by the Friday Harbor Laboratories through the Stephen and Ruth Wainwright Fellowship Endowment [to F.B. and T.N.], and the Adopt-a-Student Fund [to T.N. and S.W.].

REFERENCES

Cartamil, D. P. and Lowe, C. G. (2004). Diel movement patterns of ocean sunfish *Mola mola* off southern California. *Mar. Ecol. Prog. Ser.* **266**, 245-253.

Clark, T. D., Sandblom, E., Hinch, S. G., Patterson, D. A., Frappell, P. B. and Farrell, A. P. (2010). Simultaneous biologging of heart rate and acceleration, and their relationships with energy expenditure in free-swimming sockeye salmon (*Oncorhynchus nerka*). *J. Comp. Physiol. B* **180**, 673-684.

Domenici, P. and Blake, R. W. (1997). The kinematics and performance of fish fast-start swimming. *J. Exp. Biol.* **200**, 1165-1178.

Domenici, P., Standen, E. M. and Levine, R. P. (2004). Escape manoeuvres in the spiny dogfish (*Squalus acanthias*). *J. Exp. Biol.* **207**, 2339-2349.

Føre, M., Alfredsen, J. A. and Gronningsater, A. (2011). Development of two telemetry-based systems for monitoring the feeding behavior of Atlantic salmon (*Salmo salar* L.) in aquaculture sea-cages. *Comput. Electron. Agric.* **76**, 240-251.

Gleiss, A. C., Norman, B., Liebsch, N., Francis, C. and Wilson, R. P. (2009). A new prospect for tagging large free-swimming sharks with motion-sensitive data-loggers. *Fish. Res.* **97**, 11-16.

Gleiss, A. C., Dale, J. J., Holland, K. N. and Wilson, R. P. (2010). Accelerating estimates of activity-specific metabolic rate in fish: testing the applicability of acceleration data loggers. *J. Exp. Mar. Biol. Ecol.* **385**, 85-91.
Gleiss, A. C., Norman, B. and Wilson, R. P. (2011). Moved by that sinking feeling: variable diving geometry underlies movement strategies in whale sharks. *Funct. Ecol.* **25**, 595-607.
Goldbogen, J. A., Calambokidis, J., Oleson, E., Potvin, J., Pyenson, N. D., Schorr, G. and Shadwick, R. E. (2011). Mechanics, hydrodynamics and energetics of blue whale lunge feeding: efficiency dependence on krill density. *J. Exp. Biol.* **214**, 131-146.
Goolish, E. M. (1991). Aerobic and anaerobic scaling in fish. *Biol. Rev. Camb. Philos. Soc.* **66**, 33-56.
Halsey, L. G., Green, J. A., Wilson, R. P. and Frappell, P. B. (2009). Accelerometery to estimate energy expenditure during activity: best practice with data loggers. *Physiol. Biochem. Zool.* **82**, 396-404.
Harper, D. G. and Blake, R. W. (1989). A critical analysis of the use of high-speed film to determine maximum accelerations of fish. *J. Exp. Biol.* **142**, 465-471.
Harper, D. G. and Blake, R. W. (1991). Prey capture and the fast-start performance of northern pike *Esox lucius. J. Exp. Biol.* **155**, 175-192.
Kawabe, R., Nashimoto, K., Hiraishi, T., Naito, Y. and Sato, K. (2003a). A new device for monitoring the activity of freely swimming flatfish, Japanese flounder *Paralichthys olivaceus. Fish. Sci.* **69**, 3-10.
Kawabe, R., Kawano, T., Nakano, N., Yamashita, N., Hiraishi, T. and Naito, Y. (2003b). Simultaneous measurement of swimming speed and tail beat activity of free-swimming rainbow trout *Oncorhynchus mykiss* using an acceleration data-logger. *Fish. Sci.* **69**, 959-965.
Murchie, K. J., Cooke, S. J., Danylchuk, A. J. and Suski, C. D. (2011). Estimates of field activity and metabolic rates of bonefish (*Albula vulpes*) in coastal marine habitats using acoustic tri-axial accelerometer transmitters and intermittent-flow respirometry. *J. Exp. Mar. Biol. Ecol.* **396**, 147-155.
O'Toole, A. C., Murchie, K. J., Pullen, C., Hanson, K. C., Suski, C. D., Danylchuk, A. J. and Cooke, S. J. (2010). Locomotory activity and depth distribution of adult great barracuda (*Sphyraena barracuda*) in Bahamian coastal habitats determined using acceleration and pressure biotelemetry transmitters. *Mar. Freshw. Res.* **61**, 1446-1456.
Oppenheim, A. V., Schafer, R. W. and Buck, J. R. (1989). *Discrete-Time Signal Processing.* Englewood Cliffs, NJ: Prentice-Hall, Inc.
Payne, N. L., Gillanders, B. M., Seymour, R. S., Webber, D. M., Snelling, E. P. and Semmens, J. M. (2011). Accelerometry estimates field metabolic rate in giant Australian cuttlefish *Sepia apama* during breeding. *J. Anim. Ecol.* **80**, 422-430.
Ropert-Coudert, Y. and Wilson, R. P. (2004). Subjectivity in bio-logging science: do logged data mislead? *Mem. Natl. Inst. Polar Res.* **58**, 23-33.
Sabin, W. E. (2008). *Discrete-Signal Analysis and Design.* Hoboken, NJ: Wiley-Interscience.
Sakamoto, K.Q., Sato, K., Ishizuka, M., Watanuki, Y., Takahashi, A., Daunt, F. and Wanless, S. (2009). Can ethograms be automatically generated using body acceleration data from free ranging brids? *PLoS ONE* **4**, e5379.
Sato, K., Watanuki, Y., Takahashi, A., Miller, P. J. O., Tanaka, H., Kawabe, R., Ponganis, P. J., Handrich, Y., Akamatsu, T., Watanabe, Y. et al. (2007). Stroke frequency, but not swimming speed, is related to body size in free-ranging seabirds, pinnipeds and cetaceans. *Proc. Biol. Sci.* **274**, 471-477.
Tanaka, H., Takagi, Y. and Naito, Y. (2001). Swimming speeds and buoyancy compensation of migrating adult chum salmon *Oncorhynchus keta* revealed by speed/depth/acceleration data logger. *J. Exp. Biol.* **204**, 3895-3904.
Tsuda, Y., Kawabe, R., Tanaka, H., Mitsunaga, Y., Hiraishi, T., Yamamoto, K. and Nashimoto, K. (2006). Monitoring the spawning behavior of chum salmon with an acceleration data logger. *Ecol. Freshw. Fish* **15**, 264-274.
Webb, P. W. (1976). The effect of size on the fast-start performance of rainbow trout *Salmo gairdneri*, and a consideration of piscivorous predator-prey interactions. *J. Exp. Biol.* **65**, 157-177.
Webb, P. W. (1978). Fast-start performance and body form in seven species of teleost fish. *J. Exp. Biol.* **74**, 311-326.
Whitney, N. M., Papastamatiou, Y. P., Holland, K. N. and Lowe, C. G. (2007). Use of an acceleration data logger to measure diel activity patterns in captive whitetip reef sharks, *Triaenodon obesus. Aquat. Living Resour.* **20**, 299-305.
Whitney, N. M., Pratt, H. L., Jr, Pratt, T. C. and Carrier, J. C. (2010). Identifying shark mating behavior using three-dimensional acceleration loggers. *Endanger. Species Res.* **10**, 71-82.
Wilson, R. P., White, C. R., Quintana, F., Halsey, L. G., Liebsch, N., Martin, G. R. and Butler, P. J. (2006). Moving towards acceleration for estimates of activity-specific metabolic rate in free-living animals: the case of the cormorant. *J. Anim. Ecol.* **75**, 1081-1090.

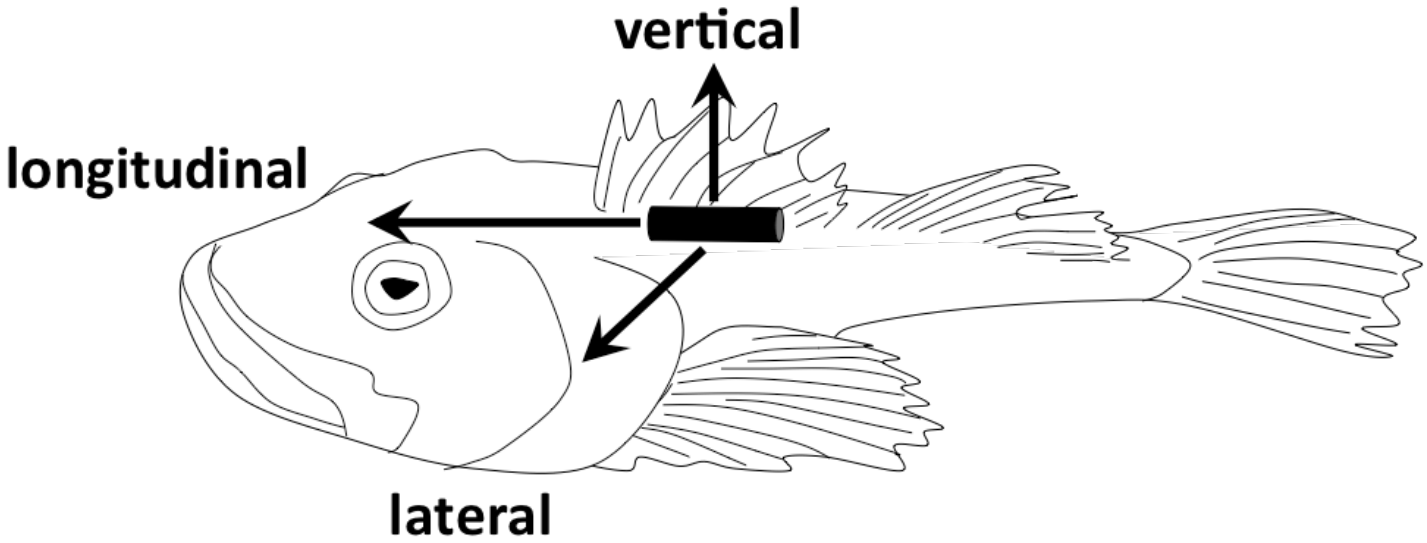

Fig. S1. Schematic representation of a sculpin with a Petersen Disk tag mounted with a tri-axial accelerometer showing the orientation of the lateral (*x*), longitudinal (*y*) and vertical (*z*) axes.

Table S1. Summary of differences (*P*) in the Φ parameter in detecting spontaneous (S) and fast-start (FS) events (Fig. 2), and in the ω_1 through ω_6 parameters in detecting feeding (F) and escape (E) activities (Fig. 3), all based on the number (*N*) of events and activities in the entire event data

Parameter	AD test statistic (*A*) (N_{DS}=70, N_{DE}=82, N_{DF}=105)	WSR (*V*) and Student's (*t*) test statistics
Φ	P_{FS}<0.05 (*A*=1.5)	$E[\sigma_{MA,S}]=E[\sigma_{MA,FS}]$
	P_S<0.05 (*A*=2.5)	*V*=108, *P*<0.001
ω_1	P_E=0.11 (*A*=0.62)	$E[\omega_{1,F}]=E[\omega_{1,E}]$
	P_F=0.83 (*A*=0.22)	*P*<0.001 (d.f.=159, *t*=10.3)
ω_2	P_E=0.2 (*A*=0.51)	$E[\omega_{2,F}]=E[\omega_{2,E}]$
	P_F=0.4 (*A*=0.38)	*P*<0.001 (d.f.=183, *t*=8.13)
ω_3	P_E=0.09 (*A*=0.64)	$E[\omega_{3,F}]=E[\omega_{3,E}]$
	P_F=0.14 (*A*=0.57)	*P*<0.001 (d.f.=177, *t*=9.21)
ω_4	P_E=0.56 (*A*=0.31)	$E[\omega_{4,F}]=E[\omega_{4,E}]$
	P_F=0.07 (*A*=0.70)	*P*<0.001 (d.f.=185, *t*=9.02)
ω_5	P_E<0.05 (*A*=1.5)	$E[\omega_{5,F}]=E[\omega_{5,E}]$
	P_F=0.22 (*A*=0.48)	*V*=3526, *P*<0.05
ω_6	P_E<0.05 (*A*=1.3)	$E[\omega_{6,F}]=E[\omega_{6,E}]$
	P_F=0.01 (*A*=0.97)	*V*=3795, *P*<0.001

Student's *t*-test (*t*) with degrees of freedom (d.f.) was used if the data were normal, based on the Anderson–Darling (AD) test (*A*), and the Wilcoxon signed-rank (WSR) test (*V*) was used otherwise, where $E[\cdot]$ represents the expected parameter values tested.